

# A reassessment of copper(II) binding in the full-length prion protein

Mark A. WELLS\*, Graham S. JACKSON†, Samantha JONES†, Laszlo L. P. HOSSZU\*†, C. Jeremy CRAVEN\*, Anthony R. CLARKE†, John COLLINGE† and Jonathan P. WALTHO\*<sup>1</sup>

\*Krebs Institute for Biomolecular Research, Department of Molecular Biology and Biotechnology, University of Sheffield, Sheffield S10 2TN, U.K., and †MRC Prion Unit, Department of Neurodegenerative Disease, Institute of Neurology, University College London, Queen Square, London WC1N 3BG, U.K.

It has been shown previously that the unfolded N-terminal domain of the prion protein can bind up to six Cu<sup>2+</sup> ions *in vitro*. This domain contains four tandem repeats of the octapeptide sequence PHGGGWGQ, which, alongside the two histidine residues at positions 96 and 111, contribute to its Cu<sup>2+</sup> binding properties. At the maximum metal-ion occupancy each Cu<sup>2+</sup> is co-ordinated by a single imidazole and deprotonated backbone amide groups. However two recent studies of peptides representing the octapeptide repeat region of the protein have shown, that at low Cu<sup>2+</sup> availability, an alternative mode of co-ordination occurs where the metal ion is bound by multiple histidine imidazole groups. Both modes of binding are readily populated at pH 7.4, while mild acidification to pH 5.5 selects in favour of the low occupancy, multiple imidazole binding mode. We have used NMR to resolve how Cu<sup>2+</sup> binds to the full-length prion protein under

mildly acidic conditions where multiple histidine co-ordination is dominant. We show that at pH 5.5 the protein binds two Cu<sup>2+</sup> ions, and that all six histidine residues of the unfolded N-terminal domain and the N-terminal amine act as ligands. These two sites are of sufficient affinity to be maintained in the presence of millimolar concentrations of competing exogenous histidine. A previously unknown interaction between the N-terminal domain and a site on the C-terminal domain becomes apparent when the protein is loaded with Cu<sup>2+</sup>. Furthermore, the data reveal that sub-stoichiometric quantities of Cu<sup>2+</sup> will cause self-association of the prion protein *in vitro*, suggesting that Cu<sup>2+</sup> may play a role in controlling oligomerization *in vivo*.

Key words: Copper (II), fluorescence, metal binding, NMR, prion, prion protein (PrP).

## INTRODUCTION

Prion diseases are a group of fatal neurodegenerative disorders that includes Creutzfeldt–Jakob disease in humans, scrapie in sheep and bovine spongiform encephalopathy in cattle. In humans such diseases can arise sporadically, be inherited or occur through infection with prion-contaminated material [1,2]. The ‘protein only’ hypothesis states that the particles that cause infection, termed prions, are composed principally or entirely of a misfolded isoform of a host-encoded protein, termed the PrP (prion protein) [3–5], with prion propagation occurring by conformational conversion of the normal cellular isoform, PrP<sup>C</sup> (cellular prion protein isoform) to the disease related isoform PrP<sup>Sc</sup> [pathogenic (scrapie) isoform of prion protein]. Mammalian PrP<sup>C</sup> is a glycolipid anchored cell surface glycoprotein found at high levels in the central nervous system, lymphatic tissue, activated lymphocytes and at neuromuscular junctions [6]. The physiological function of PrP remains unclear; ablation of the *Prn-P* gene in mice results in viable animals without gross developmental or behavioral abnormalities [7], although more detailed studies revealed some phenotypic effects, including altered synaptic physiology [8]. Biophysical and biochemical studies have demonstrated that PrP specifically binds Cu<sup>2+</sup>, and this has led to the proposal that PrP is a metalloprotein *in vivo* [9–21].

PrP<sup>C</sup> comprises a flexibly disordered N-terminal domain (residues 23–125) [22] and a globular, mainly  $\alpha$ -helical, C-terminal domain (residues 126–231) [23]. Residues 60–91 of the protein comprise four tandem repeats of the sequence PHGGGWGQ.

It is this region, known as the octapeptide repeats, which was first discovered to bind Cu<sup>2+</sup> [10,11], and a considerable body of work has since been devoted to identifying the number of binding sites, their affinities and the nature of co-ordination in both the octapeptide repeats and the full-length prion protein, PrP<sup>23–231</sup> [9,12–21]. Until recently, the accepted model of Cu<sup>2+</sup> binding to the full-length prion protein, at pH 7.4, was that it binds six Cu<sup>2+</sup> ions at separate sites, one in each of the four octapeptide repeats and at two additional sites involving His<sup>96</sup> and His<sup>111</sup>, and each with co-ordination from a single histidine imidazole group and amide nitrogen atoms from nearby glycine residues [19].

Two recent studies have shown that the model described above provides an incomplete picture of Cu<sup>2+</sup> binding in the prion protein, by demonstrating that a peptide representing the four octapeptide repeats displays multiple modes of Cu<sup>2+</sup> binding at pH 7.4 [24,25]. The peptide can bind a single Cu<sup>2+</sup> ion through multiple histidine co-ordination; however, in the presence of more Cu<sup>2+</sup>, binding of up to four Cu<sup>2+</sup> ions occurs, with all of these co-ordinated in identical sites – each involving deprotonated backbone amide nitrogen atoms and a single histidine residue. Perhaps counter-intuitively, these four Cu<sup>2+</sup> binding sites replace a single site of higher affinity. Peptides representing the octapeptide repeats cannot, however, be considered a complete model for Cu<sup>2+</sup> binding to the prion protein. Cu<sup>2+</sup> binding sites outside the octapeptide repeats have also been reported, involving His<sup>96</sup> and His<sup>111</sup> [12,19,26,27]. It is thus clear that, to fully understand the binding of Cu<sup>2+</sup> to the prion protein, binding to the full-length protein needs to be investigated, and in particular the involvement of multiple histidine–Cu<sup>2+</sup> co-ordination events. Given the low

Abbreviations used: GdnHCl, guanidinium chloride; HSQC, heteronuclear single quantum coherence; p.p.m., parts per million; PrP, prion protein; PrP<sup>C</sup>, cellular prion protein isoform; PrP<sup>Sc</sup>, pathogenic (scrapie) isoform of prion protein; PrP–Cu<sup>2+</sup>, complex of the full-length prion protein with one Cu<sup>2+</sup> ion; PrP–2Cu<sup>2+</sup>, complex of the full-length prion protein with two Cu<sup>2+</sup> ions.

<sup>1</sup> To whom correspondence should be addressed (email j.waltho@sheffield.ac.uk).

availability of  $\text{Cu}^{2+}$  in the extracellular milieu (examined in more detail in the Discussion), this higher-affinity binding mode is more likely to be substantially populated *in vivo*.

Although the full-length prion protein is poorly soluble above pH 6 [22], it can, fortunately, be studied at lower pH values where multiple histidine– $\text{Cu}^{2+}$  co-ordination events should be favoured. In aqueous solution,  $\text{H}^+$  ions compete for the basic co-ordinating groups that form a metal binding site, and thus the  $\text{p}K_a$  of the co-ordinating groups and the pH of the solution are both determinants of the stability of a metal complex. The  $\text{p}K_a$  of the histidine imidazole group is around 6, which is substantially lower than that of a backbone amide nitrogen, and thus co-ordination by multiple histidines will be maintained at lower pH compared with co-ordination modes involving deprotonated backbone amide groups. We find that binding of two  $\text{Cu}^{2+}$  ions is maintained in the full-length prion protein at pH 5.5, and we have also investigated the nature of the co-ordination in this complex. Here we report the locations of these binding sites and the identity of the co-ordinating groups. We demonstrate that these binding sites are of sufficient affinity to be maintained in the presence of substantial concentrations of exogenous histidine, which is known to bind  $\text{Cu}^{2+}$  *in vivo* [28]. Finally, we show how  $\text{Cu}^{2+}$  binding is altered in a truncated form of PrP, comprising residues 91–231 (PrP<sup>91–231</sup>), which lacks the octapeptide repeat regions, but which can still transmit infection.

## EXPERIMENTAL

### Expression, purification and metal stripping of PrP<sup>91–231</sup>

Human PrP<sup>91–231</sup>, with a methionine residue at position 129, was expressed and purified as described previously [29,30]. The PrP<sup>23–231</sup> and PrP<sup>91–231</sup> constructs used here both have the additional three-residue sequence SFR present at the N-terminus, which forms part of the thrombin cleavage site. To ensure the protein was free of metal ions, the protein was repeatedly buffer exchanged with 8 M urea, 20 mM EDTA, 25 mM Tris/acetate, pH 8.0, and then refolded by dilution in 5 mM Mes, pH 5.5, in an Amicon ultrafiltration unit (3 kDa molecular mass cut-off). The protein concentration for refolding was less than 1 mg/ml. All buffers used during and after the metal stripping step were prepared using, wherever possible, Aristar grade reagents. In addition all buffers were made using AnalR grade water and treated with Chelex resin (Bio-Rad Laboratories).

### Expression, purification and metal stripping of full-length prion protein, PrP<sup>23–231</sup>

Full-length human prion protein, with a methionine residue at position 129, was expressed with an N-terminal His<sub>6</sub>-tag containing a thrombin cleavage site, using standard molecular biology protocols. Expression of uniformly <sup>15</sup>N and <sup>13</sup>C labelled protein and the initial purification by Ni<sup>2+</sup>-nitrilotriacetate chromatography was carried out using the same procedures described previously for PrP<sup>91–231</sup> [29,30]. Oxidation of the disulfide bond was checked by HPLC [30] and was complete after 24 h without the aid of a catalyst. The protein was diluted to less than 1 mg/ml in 6 M GdnHCl (guanidinium chloride) and 50 mM Tris/HCl, pH 8.0, and then refolded by dialysis against 150 mM acetate/Tris and 0.02 % NaN<sub>3</sub>, pH 3.5. In preparation for the thrombin cleavage step, the pH was gradually increased by successive dialysis steps against 10 mM Tris/acetate and 0.02 % NaN<sub>3</sub> at pH 4.5, 5.5, 6.5 and 7.0. The fusion protein was cleaved by 0.6 units of thrombin (Novagen) per mg of protein with 2.5 mM CaCl<sub>2</sub>. The reaction mixture was incubated at 37 °C for 24 h.

Cleavage was halted by the addition of the Complete™ protease inhibitor cocktail (Roche). For the final purification step a higher pH was required and this had to be carried out under denaturing conditions for the protein to be soluble. Urea was added to the reaction mixture to a final concentration of 8 M and the pH was adjusted to 7.5. The denatured protein solution was then loaded on to an SP-Sepharose™ Fast Flow column (Amersham), pre-equilibrated with equilibration buffer (8 M urea, 150 mM NaCl and 50 mM Tris/HCl, pH 7.5). The column was washed extensively with the equilibration buffer. A salt gradient from 150 to 600 mM NaCl in 8 M urea, 50 mM Tris/HCl, pH 7.5 was run over 8 column volumes and the protein was eluted by approx. 300–400 mM NaCl. To remove any metal ions, the purified protein was repeatedly buffer exchanged against 8 M urea, 25 mM EDTA and 20 mM Tris/acetate, pH 8.0, and then refolded by dilution in 150 mM acetate/Tris, pH 3.5, in an Amicon ultra-filtration unit (3 kDa molecular mass cut-off). The protein concentration for refolding was less than 1 mg/ml. The buffer was exchanged to 20 mM acetate/TRIS pH 4.5 and then finally 10 mM Mes pH 5.5. All buffers used during and after the metal stripping step were prepared using, wherever possible, Aristar grade reagents. In addition all buffers were made using AnalR grade water and treated with Chelex resin (BioRad Laboratories).

### NMR sample preparation

For backbone and side-chain assignment experiments, metal-free full-length prion protein in 20 mM Mes, pH 5.5 was concentrated to approx. 1 mM. NaN<sub>3</sub> (to a final concentration of 1 mM), EDTA-free Complete™ protease inhibitor (Roche) and 10 % <sup>2</sup>H<sub>2</sub>O were added, and the pH readjusted to 5.5 by the addition of Mes. The final Mes concentration was approx. 30 mM. The sample was centrifuged at 16000 g for 5 min to remove any precipitated material. For titrations with  $\text{Cu}^{2+}$  the samples were prepared in the same way with the following exceptions, the protein was concentrated to approx. 0.5 mM or 0.1 mM and no NaN<sub>3</sub> was added. An absorbance measurement at 280 nm was taken on an aliquot of the sample diluted into 6 M GdnHCl and 50 mM Tris/HCl, pH 8.0. The protein concentration was determined on the basis a calculated molar absorption coefficient [31]. Inductively coupled plasma MS analysis showed that no significant quantities of transition metals were present in the NMR sample (transition metals above 1 μM were: Cd, 5.5 μM; Cu, 4.7 μM; Zn, 3.6 μM; and Fe, 1.8 μM). For titration with  $\text{Cu}^{2+}$ , a sample of 1.2 mM PrP<sup>91–231</sup> was prepared in 5 mM Mes, pH 5.5, with 10 % <sup>2</sup>H<sub>2</sub>O. Measurement of the protein concentration was carried out by the method described above. Nitric acid washed NMR tubes were used for metal titration samples.

### NMR resonance assignment experiments for the full-length prion protein

See online Supplementary Materials and methods at <http://www.BiochemJ.org/bj/399/bj3990435add.htm> for details.

### Cu<sup>2+</sup> titrations monitored by NMR

The PrP<sup>91–231</sup> sample was titrated with four aliquots of 4 mM CuSO<sub>4</sub>, 10 mM glycine and 5 mM Mes, pH 5.5, to give molar fractions of  $\text{Cu}^{2+}$  relative to protein of 0.25, 0.50, 0.75 and 1.00. NMR spectra were recorded at 303 K on a Bruker Avance DRX-600 spectrometer. At each point in the titration a <sup>1</sup>H<sup>15</sup>N HSQC (heteronuclear single quantum coherence) and aromatic and aliphatic <sup>1</sup>H<sup>13</sup>C HSQCs were recorded. The full-length prion protein sample was titrated with 13 aliquots of 4 mM CuSO<sub>4</sub>, 10 mM glycine and 5 mM Mes, pH 5.5, to give molar fractions of

Cu<sup>2+</sup> relative to protein of 0.05, 0.10, 0.20 and, in steps of 0.20, to 2.20. NMR spectra were recorded at 303 K on a Bruker Avance AV-800 spectrometer. Again at each point in the titration a <sup>1</sup>H<sup>15</sup>N HSQC and aromatic and aliphatic <sup>1</sup>H<sup>13</sup>C HSQCs were recorded.

### Determination of dissociation constants

Samples of full-length prion protein (3.5 μM) in 5 mM MES, pH 5.5, were prepared containing either 10 or 100 mM histidine. CuSO<sub>4</sub> was added as a glycine complex in 5 mM Mes at pH 5.5, to give the appropriate final Cu<sup>2+</sup> concentrations. Fluorescence measurements were made at 30 °C with an excitation wavelength of 291 nm and an emission wavelength of 345 nm, using a Jasco FP-750 spectrofluorimeter. The contribution of collisional quenching effects was evaluated by titrating samples of 20 μM *N*-acetyltryptophanamide (matching the concentration of tryptophan residues in the prion protein sample) with Cu<sup>2+</sup> under the same conditions. The prion protein data was then corrected for the measured collisional quenching effect.

Analysis of the data and least-squares curve-fitting was carried out using the Grafit program (Erithacus Software). To obtain the apparent dissociation constant for the second Cu<sup>2+</sup> binding event, the fluorescence data recorded in the presence of 10 mM histidine were fitted to a discontinuous function describing two phases of metal binding (eqns 1 and 2), where  $F_0$  is the initial fluorescence and  $F_M$  is the fluorescence at a given metal concentration,  $A_1$  and  $A_2$  are the amplitudes of the fluorescence changes associated with each event,  $M$  is the total metal concentration,  $P$  is the total protein concentration and  $K_{d2}$  is the apparent dissociation constant of the second binding event. A linear function describes the first event where the apparent  $K_d$  value is much less than the concentration of sites ( $M \leq P$ ; eqn 1), whilst the second event, for which the apparent  $K_d$  value is similar to the concentration of sites, is described by the quadratically-derived ligand binding equation ( $M > P$ ; eqn 2).

$$F_M = F_0 + M \left( \frac{A_1}{P} \right) \quad (1)$$

$$F_M = F_0 + A_1 + A_2 \left( \frac{M + K_d - \sqrt{(M + K_d)^2 - 4(M - P)P}}{2P} \right) \quad (2)$$

The data acquired in the presence of 100 mM histidine were fitted to eqn 3 which describes metal binding to a single site, with a dissociation constant of  $K_{d1}$ . The apparent  $K_d$  value of the second site, under these conditions, will be too large to make a significant contribution to the observed fluorescence quenching and hence the contribution of this site was ignored in the fitting procedure.

$$F_M = F_0 + A_1 \left( \frac{P + M + K_{d1} - \sqrt{(P + M + K_{d1})^2 - 4MP}}{2P} \right) \quad (3)$$

The true  $K_d$  values of first and second Cu<sup>2+</sup> binding events at pH 5.5 were calculated using eqn (4), where  $K_d(\text{app})$ , is the measured apparent dissociation constant,  $K_d^1(\text{His})$  and  $K_d^2(\text{His})$  are the stepwise dissociation constants for formation of a Cu(His)<sub>2</sub> complex at pH 5.5, (1.2 μM and 160 μM respectively; [30]) and the concentration of histidine is [His].

$$K_d = \frac{K_d(\text{app})K_d^1(\text{His})K_d^2(\text{His})}{[\text{His}]^2} \quad (4)$$

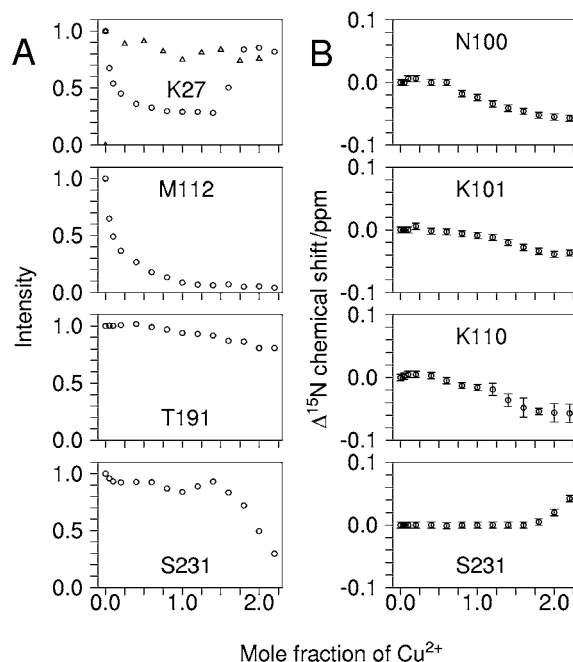


**Figure 1** Titration of full-length human prion protein with Cu<sup>2+</sup> bis-glycinate monitored by <sup>1</sup>H<sup>15</sup>N HSQC

(A) NMR signal heights for residues Lys<sup>27</sup>, Met<sup>112</sup>, Thr<sup>191</sup> and Ser<sup>231</sup>. (B) <sup>15</sup>N chemical shift changes for residues Asn<sup>100</sup>, Lys<sup>101</sup>, Lys<sup>110</sup> and Ser<sup>231</sup>. All data is from a titration of 440 μM of protein, with the exception of the data shown by triangles in the plot for Lys<sup>27</sup>, which is from a titration of 110 μM of protein.

## RESULTS

### NMR-detected effects of Cu<sup>2+</sup> addition

Observation of NMR signals as a protein is titrated with Cu<sup>2+</sup> provides a site-specific probe for the identification of nuclei close to the metal ion in a Cu<sup>2+</sup>–protein complex. Proximity to the paramagnetic Cu<sup>2+</sup> ion causes acceleration of the T<sub>2</sub> relaxation of nuclei, and hence broadens NMR signals, leading to a loss of peak height [32]. Nuclei close to the metal binding site can therefore be identified by a reduction in the height of their NMR signals as Cu<sup>2+</sup> is titrated into the protein. Backbone and side-chain signals were monitored on addition of Cu<sup>2+</sup> bisglycinate to PrP<sup>23–231</sup> using <sup>1</sup>H<sup>15</sup>N and <sup>1</sup>H<sup>13</sup>C HSQC NMR spectra. The presence of glycine allows the Cu<sup>2+</sup> to be added as a pH buffered solution by preventing the precipitation of Cu<sup>2+</sup> as Cu(OH)<sub>2</sub>, which would otherwise occur at pH 5.5 [33]. The overlap in chemical shift of the signals from the octapeptide repeat region meant that these residues were represented by a single set of resonances, each of which was a combination of four or five signals, one from each repeating unit and from a pseudo-octapeptide repeat sequence at positions 52–59.

The effects of titration with Cu<sup>2+</sup> on the height of the protein's NMR signals fall into four broad categories, of which representative examples are shown in Figure 1(A). Certain signals were almost completely unaffected, while others were initially unaffected but are attenuated after approx. 2 molar equivalents of Cu<sup>2+</sup> have been added. A third group show substantial attenuation after addition of sub-stoichiometric quantities of Cu<sup>2+</sup> and the final group behave similarly to these but begin to recover after approx. 1.4 molar equivalents of Cu<sup>2+</sup> have been added.

### The full-length prion protein binds two $\text{Cu}^{2+}$ ions at pH 5.5

Numerous backbone  $[\text{N},\text{H}^{\text{N}}]$  (Throughout 2D  $^1\text{H}^{15}\text{N}$  HSQC and  $^1\text{H}^{13}\text{C}$  HSQC crosspeaks will be referred to by giving the two coupled nuclei that produce the crosspeaks in brackets, for example  $[\text{C}\beta, \text{H}\beta]$ .) signals, for example those of  $\text{Thr}^{191}$  (Figure 1A), show very limited reduction in height throughout the titration, indicating that these residues are remote from any metal binding site. In contrast, there are a groups of signals from residues such as  $\text{Ser}^{231}$  (Figure 1A) for which, initially, the backbone  $[\text{N},\text{H}^{\text{N}}]$  signal peak heights are largely unaffected by  $\text{Cu}^{2+}$  addition but which rapidly lose height after approx. 2 molar equivalents of  $\text{Cu}^{2+}$  have been added. This behaviour occurs at multiple sites in the vicinity of residues that have a functional group with a propensity for metal binding (e.g.  $\text{His}^{140}$ ,  $\text{Asp}^{144}$ ,  $\text{Asp}^{178}$ ,  $\text{Glu}^{207}$  and  $\text{Ser}^{231}$ ). Similarly, in terms of chemical shift, some  $[\text{N},\text{H}^{\text{N}}]$  signals exhibit changes only after approx. 2 molar equivalents of  $\text{Cu}^{2+}$  have been added, including those of  $\text{Ser}^{143}$ ,  $\text{Asp}^{144}$ ,  $\text{Tyr}^{145}$  and  $\text{Ser}^{231}$  (Figure 1B). The affected residues are positioned at several distinct sites on the surface of the protein, so the effects cannot be due to a single specific  $\text{Cu}^{2+}$  binding site. Instead they are the result of several different transient interactions with  $\text{Cu}^{2+}$  ions, at separate locations on the protein's surface. The most noteworthy feature of these observations is that the NMR signals from residues involved in these  $\text{Cu}^{2+}$  binding sites are completely unaffected by the first two mole equivalents of  $\text{Cu}^{2+}$  added to the sample. The only explanation for this is that the protein completely sequesters two mole equivalents of  $\text{Cu}^{2+}$  in binding sites of substantially higher affinity. This shows that higher affinity  $\text{Cu}^{2+}$  binding in the full-length prion protein saturates at an apparent  $\text{Cu}/\text{PrP}$  stoichiometry of  $1.8 \pm 0.2$ , which is compatible with a stoichiometry of 2:1.

### Identification of the $\text{Cu}^{2+}$ co-ordinating groups in the $\text{PrP}-\text{Cu}^{2+}$ (complex of the full-length prion protein with one $\text{Cu}^{2+}$ ion) and $\text{PrP}-2\text{Cu}^{2+}$ (complex of the full-length prion protein with two $\text{Cu}^{2+}$ ions) complexes

The behaviour of the third category of NMR signals, of which  $\text{Met}^{112}$  is typical (Figure 1A), reveals the identity of the co-ordinating groups that form the two higher affinity  $\text{Cu}^{2+}$  binding sites. This group of  $[\text{N},\text{H}^{\text{N}}]$  signals show a substantial loss of peak height on addition of the first aliquots of  $\text{Cu}^{2+}$  to the sample, with complete loss of the signal occurring prior to the addition of two molar equivalents of  $\text{Cu}^{2+}$ . The largest reductions in peak heights are in signals from the six histidine residues of the N-terminal domain and from residues nearby in the sequence. Figure 2(A) shows the reductions in peak heights at a  $\text{Cu}/\text{PrP}$  stoichiometry of 1.8:1. At this stoichiometry, any reductions in peak heights due to the weaker binding sites, described above, can be eliminated. The  $^1\text{H}^{15}\text{N}$  HSQC data thus point to all six histidine residues of the N-terminal domain being involved in the formation of the higher affinity complexes. Importantly, no large changes in behaviour are observed for any of the NMR signals on passing a  $\text{Cu}/\text{PrP}$  stoichiometry of 1:1, which suggests that the first and second binding sites are not distinct from each other – a point that is discussed in more detail below. The behaviour of signals such as  $\text{Ser}^{231}$   $[\text{N},\text{H}^{\text{N}}]$  (Figure 1A), which are largely protected from attenuation by  $\text{Cu}^{2+}$  binding up to a  $\text{Cu}/\text{PrP}$  stoichiometry approaching 2:1, allows us to rule out the possibility that the effects we attribute to formation of a  $\text{Cu}^{2+}$ -protein complex are instead due to non-specific interactions with free  $\text{Cu}^{2+}$  ions.

To confirm that all six histidine residues of the N-terminal domain are the co-ordinating residues, and to determine if any additional co-ordinating groups are involved, the behavior of  $[\text{C},\text{H}]$  NMR signals on titration with  $\text{Cu}^{2+}$  was also measured. Signals

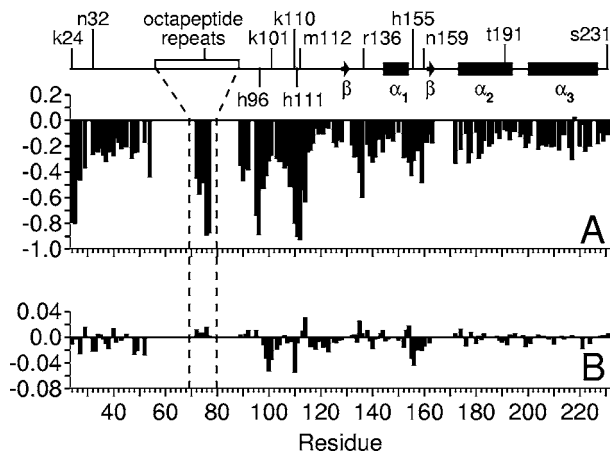


**Figure 2** Changes in the backbone  $[\text{N},\text{H}^{\text{N}}]$  NMR signals induced by  $\text{Cu}^{2+}$  binding to full-length human prion protein plotted against residue number

The degenerate octapeptide repeat signals are plotted in the order (GG)WGQ(P)HG and no data is presented for the bracketed glycine residues due to signal overlap. Signal height changes are shown as a fraction of the starting value, for the addition of 1.8 mole equivalents of  $\text{Cu}^{2+}$  bisglycinate (A). The large reductions at residues 24–25, 95–96, 110–112 and the octapeptide repeat His-Gly sequence arise from paramagnetic quenching due to the proximity of these residues to  $\text{Cu}^{2+}$  in the  $\text{PrP}(\text{Cu}^{2+})_2$  complex. (B) The  $^{15}\text{N}$  chemical shift changes after addition of 1.8 mole equivalents of  $\text{Cu}^{2+}$  bisglycinate in p.p.m.

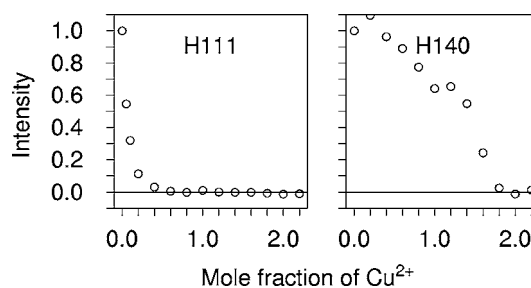


**Figure 3** Reductions in the heights of histidine side-chain  $[\text{C}\delta, \text{H}\delta]$  NMR signals induced by proximity to  $\text{Cu}^{2+}$  in  $\text{PrP}^{23-231}$

Plots show the signal height as a fraction of its starting value during titration with  $\text{Cu}^{2+}$  for  $\text{His}^{111}$  (A), part of the higher affinity binding site, and  $\text{His}^{140}$  (B), which only binds  $\text{Cu}^{2+}$  after higher affinity binding is saturated.

completely attenuated by the addition of sub-stoichiometric amounts of  $\text{Cu}^{2+}$  included the  $[\text{C}\beta, \text{H}\beta]$ ,  $[\text{C}\delta 2, \text{H}\delta 2]$  and  $[\text{C}\epsilon 1, \text{H}\epsilon 1]$  signals of  $\text{His}^{96}$ ,  $\text{His}^{111}$  and all of the octapeptide repeat histidine residues, but not those of other histidine residues such as  $\text{His}^{140}$  (Figure 3). Attenuation of signals in this way is expected for nuclei that are close to  $\text{Cu}^{2+}$  in a protein complex, where the exchange rate of  $\text{Cu}^{2+}$  between protein molecules is fast on an NMR timescale (i.e. where the dissociation rate exceeds the chemical-shift change induced by binding in Hz). Thus all six histidines (i.e. four from the octapeptide repeats plus  $\text{His}^{96}$  and  $\text{His}^{111}$ ) must co-ordinate  $\text{Cu}^{2+}$  in the  $\text{PrP}(\text{Cu}^{2+})_1$  complex, and exchange on a 10 ms or faster timescale. The only other signals reduced in the same fashion were the  $[\text{C}\alpha, \text{H}\alpha]$  and  $[\text{C}\beta, \text{H}\beta]$  signals from the N-terminal  $\text{Ser}^{20}$ , which is the first of the three residues added to the N-terminus of the full-length prion protein sequence to form a thrombin cleavage site. The N-terminal amine is thus also a co-ordinating group. The hydroxy group of  $\text{Ser}^{20}$  may be an additional ligand, though the affinity of this group for  $\text{Cu}^{2+}$  is predicted to be orders of magnitude weaker than that of the amine [34,35].

In summary, the data indicate that at least seven functional groups (the six histidine residues of the N-terminal domain and the N-terminal amine) contribute to co-ordinating a single  $\text{Cu}^{2+}$  ion in the  $\text{PrP}(\text{Cu}^{2+})_1$  complex.  $\text{Cu}^{2+}$  generally co-ordinates with three, four or five groups in proteins (<http://metallo.scripps.edu/PROMISE/CUMAIN.html>), and hence these seven co-ordinating groups cannot all be simultaneously involved in a single  $\text{Cu}^{2+}$  complex. The higher-affinity  $\text{Cu}^{2+}$  binding in the full-length prion protein must instead be derived from a rapidly exchanging ensemble of different co-ordination geometries, each of which has comparable stability, involving different combinations of the seven co-ordinating groups.

On increasing the  $\text{Cu}/\text{PrP}$  stoichiometry beyond 1:1, no new protein signals become substantially broadened until the second binding site is saturated. Therefore, the second binding site must be formed from a subset of the co-ordinating groups that take part in the ensemble of binding modes, which collectively form the highest-affinity site.

### Self-association of the $\text{PrP}-\text{Cu}^{2+}$ complex

In the fourth group of NMR signals another distinct behaviour is observed, peak height is initially reduced by the addition of  $\text{Cu}^{2+}$  but the signals recover towards their initial height as a  $\text{Cu}/\text{PrP}$  stoichiometry of 2:1 is approached (e.g. those of residue Lys<sup>27</sup> in Figure 1A). This group of  $[\text{N},\text{H}^{\text{N}}]$  signals includes those from residues in several stretches of the N-terminal domain, namely: 24–48, 100–108 and 125–126. When the experiment was repeated with the protein concentration reduced from 440  $\mu\text{M}$  to 110  $\mu\text{M}$  (Lys<sup>27</sup>; Figure 1A), signals in this group were not dramatically affected by the addition of  $\text{Cu}^{2+}$ , indicating that their behaviour at the higher protein concentration must be caused by an intermolecular process. Thus at sub-saturating levels of  $\text{Cu}^{2+}$  and 440  $\mu\text{M}$  protein, a self-associated form of the prion protein must be at least transiently present. Concentration dependent effects are confined to the disordered N-terminal domain and thus show that it is this section of the protein that self-associates. The most probable cause of this self-association is that metal ions are readily co-ordinated by histidine side-chains from more than one protein molecule, since the concentration of the protein and the effective concentration of histidine residues in the same chain are likely to be similar. This self-associated protein species causes an acceleration of the relaxation of the nuclei in residues such as Lys<sup>27</sup>, either by placing them in closer proximity to the  $\text{Cu}^{2+}$  ion or through localized increases in the correlation time. At a  $\text{Cu}/\text{PrP}$  stoichiometry of 1.8:1, where these signals have fully recovered, we can infer that no significant amount of the self-associated species remains. At this point in the titration the effects on signals that arise solely from proximity to  $\text{Cu}^{2+}$  in the monomer can therefore be clearly distinguished and are illustrated in Figure 2(A).

### Chemical-shift changes in the $\text{PrP}-\text{Cu}^{2+}$ and $\text{PrP}-2\text{Cu}^{2+}$ complexes

Large chemical-shift changes were not observed on formation of either  $\text{PrP}-\text{Cu}^{2+}$  or  $\text{PrP}-2\text{Cu}^{2+}$  complexes, indicating that the electronic environment for the paramagnetic ion must be close to isotropic in both cases [37]. However, smaller chemical-shift changes of less than 0.1 p.p.m. (parts per million) in the <sup>15</sup>N dimension and less than 0.02 p.p.m. in the <sup>1</sup>H dimension are present, confirming the rapid exchange of  $\text{Cu}^{2+}$  between prion protein molecules. The distribution of <sup>15</sup>N chemical-shift changes for the  $\text{PrP}-2\text{Cu}^{2+}$  complex is plotted in Figure 2(B). Certain signals change in chemical shift up to a  $\text{Cu}/\text{PrP}$  stoichiometry of approx. 2:1 and then stop. This saturable behaviour shows that these chemical-shift changes must be associated with the formation of

the  $\text{PrP}-\text{Cu}^{2+}$  and  $\text{PrP}-2\text{Cu}^{2+}$  complexes. The largest shift changes in this category are seen in signals from residues in the region between His<sup>96</sup> and His<sup>111</sup> (for example Asn<sup>100</sup>, Lys<sup>101</sup> and Lys<sup>110</sup> in Figure 1B), plus some from residues in the first helix (namely His<sup>155</sup> and Arg<sup>156</sup>) and at the N-terminus (namely Lys<sup>24</sup>, Arg<sup>25</sup> and Lys<sup>27</sup>). Similar but less substantial changes are seen in signals from other residues close to the N-terminus and a few residues near His<sup>155</sup> and Arg<sup>156</sup> in the C-terminal domain. The locations of these chemical-shift changes do not correlate with the changes in peak height, for example the height of signals like Lys<sup>101</sup> and Asn<sup>100</sup> are not substantially affected by  $\text{Cu}^{2+}$  binding, so these changes are unlikely to be a direct result of proximity to  $\text{Cu}^{2+}$ . The shifts observed in the region between His<sup>96</sup> and His<sup>111</sup> (Figure 2B) are most likely reporting a conformational redistribution associated with the formation of a partially ordered loop between these residues. However the lack of substantial <sup>1</sup>H chemical-shift-dispersion in the  $\text{PrP}-\text{Cu}^{2+}$  and the  $\text{PrP}-2\text{Cu}^{2+}$  complexes indicates  $\text{Cu}^{2+}$  binding does not bring about a highly ordered, side-chain-immobilized structure in the N-terminal domain of the full-length prion protein. Instead,  $\text{Cu}^{2+}$  binding at this second site uses the excess metal co-ordinating residues present in the ensemble of  $\text{PrP}-\text{Cu}^{2+}$  complexes to produce a poorly ordered structure.

### Interaction of the $\text{Cu}^{2+}$ binding site with the C-terminal domain

Although the C-terminal domain does not contribute directly to  $\text{Cu}^{2+}$  co-ordination at the higher-affinity site, the heights of certain  $[\text{N},\text{H}^{\text{N}}]$  NMR signals from the C-terminal domain are substantially reduced in the  $\text{PrP}-2\text{Cu}^{2+}$  complex. The largest of these reductions map to a region of the protein surface formed by residues close to the C-terminal end of helix 1 (His<sup>155</sup> and Asn<sup>159</sup>) and the nearby loop between the first  $\beta$ -strand and helix 1 (Ser<sup>135</sup> and Arg<sup>136</sup>; Figure 4A). The reductions can be explained if this area of the C-terminal domain surface comes into close proximity with the section of the N-terminal domain that co-ordinates  $\text{Cu}^{2+}$ . An alternative explanation, where these reductions in peak height were due to direct weak  $\text{Cu}^{2+}$  binding at a site on the C-terminal domain can be eliminated. In this scenario the reductions in signal height would be expected to become more dramatic after the higher-affinity  $\text{Cu}^{2+}$  binding was saturated, in the same way as is seen at the Ser<sup>231</sup>  $[\text{N},\text{H}^{\text{N}}]$  signal (Figure 1A). This does not happen and instead the changes stop at the 2:1 point of the titration showing that they must be related to the saturable higher-affinity binding.

Chemical-shift changes are also observed for the same section of helix 1 (Figure 2B), arising either from the interaction between domains forming in a  $\text{Cu}^{2+}$  dependent fashion, or from  $\text{Cu}^{2+}$  binding to a region of the N-terminus, which was already interacting with the C-terminal domain. Strikingly, the changes observed for full-length prion protein,  $\text{PrP}^{23-231}$ , bound to two  $\text{Cu}^{2+}$  ions are very similar to the changes we observe for the truncated construct  $\text{PrP}^{91-231}$  bound to a single  $\text{Cu}^{2+}$  in the same conditions (Figure 4B; experiments on this construct are discussed in more detail below). Since signals for residues 115–134 are not greatly affected by  $\text{Cu}^{2+}$  binding, the sequence responsible for the interaction with the C-terminal domain must lie between the residues at positions 91 and 114.

### Measurement of $\text{Cu}^{2+}$ binding affinity

There are two highly specific  $\text{Cu}^{2+}$  binding events in the full-length prion protein that are apparent from the NMR observations. These events can be monitored at much lower protein concentration by measuring the quenching of the intrinsic tryptophan fluorescence, revealing that the two sites have significantly different affinities. In these experiments, the apparent affinities of the two metal binding events are reduced to measurable values by

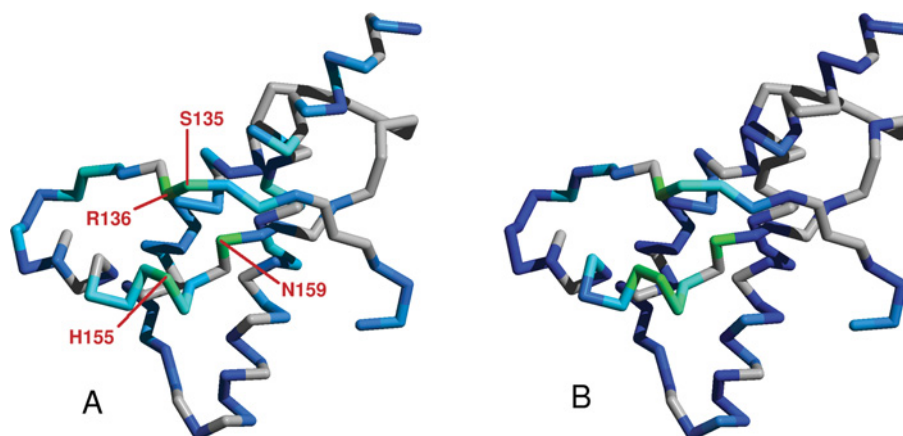


**Figure 4** The  $\text{Cu}^{2+}$ -bound N-terminal domain contacts the C-terminal domain

The reductions in the heights of backbone  $[\text{N}, \text{H}^{\text{N}}]$  signals in the C-terminal domain of PrP, induced by proximity to the  $\text{Cu}^{2+}$  bound to the N-terminal domain, are illustrated on the backbone structure by a colour scale, ranging from dark blue to cyan (0–30% peak height reduction) and cyan to green (30–60% reduction). Data is shown for the full-length prion protein loaded with two  $\text{Cu}^{2+}$  ions (**A**) and the truncated PrP<sup>91–231</sup> construct, loaded with one  $\text{Cu}^{2+}$  ion (**B**). Residues for which there are no data are coloured grey. Signals from the area of the C-terminal domain that contacts the unfolded N-terminal domain see the largest reductions (coloured green) because they are closer to the  $\text{Cu}^{2+}$  ion bound to the unfolded domain. The unfolded domain of the protein and the  $\text{Cu}^{2+}$  ion bound to it are omitted for clarity.

the inclusion of a competitive chelator that competes for free metal ions. With knowledge of the affinity of the competition reagent for the metal, a true dissociation constant for the protein can be calculated from the measured apparent dissociation constant. The affinities of both sites were measured using competition by histidine, which forms a  $\text{Cu}^{2+}$ –bischistidinate complex. The affinity of the second of the two  $\text{Cu}^{2+}$  binding sites was measured in the presence of 10 mM histidine. Under these conditions, fluorescence quenching was linear to a stoichiometry of 1:1, indicating that the first binding event was at the strong binding limit. Throughout, we use ‘strong binding’ to describe a situation where the dissociation constant is much less than the concentration of binding sites and ‘weak binding’ for situations where it is similar to or greater than the concentration of sites. Weak binding is a condition necessary for measuring a dissociation constant in a titration experiment. In contrast, the second binding event had a measurable apparent dissociation constant of  $6 \mu\text{M}$  (Figure 5A), showing that the affinities of the two binding events are not equal, as might be predicted from the similarity of the co-ordinating groups in each. To reduce the apparent affinity of the first site to a measurable value it was necessary to use competition with 100 mM histidine. Under these conditions an apparent dissociation constant of  $4 \mu\text{M}$  was measured, with no initial strong binding phase (Figure 5B). In combination, these fluorescence data also show that the first and second binding events are not co-operative, since the data shown in Figures 1(A) and 1(B) are not compatible with a single dissociation constant process.

The absolute affinity of histidine for  $\text{Cu}^{2+}$  can be used to calculate the affinity at pH 5.5 [30] and using this information we can make estimates of the true dissociation constants for the two binding events in the full-length prion protein at this pH. The interpretation of these competition experiments is, however, ambiguous, because it is not known if the protein is interacting with a  $\text{Cu}^{2+}$  ion or a  $\text{Cu}^{2+}$ –monohistidinate complex. If the second binding event in the protein involves a  $\text{Cu}^{2+}$ –mono-histidinate complex,  $\log_{10}(K_d/M)$  for the  $\text{Cu}^{2+}$ –histidine–protein complex would be  $-7.0 \pm 0.4$ , however if the protein is binding a free  $\text{Cu}^{2+}$  ion then the  $\log_{10}(K_d/M)$  has a value of  $-10.8 \pm 0.4$  (the  $K_d$  values calculated here are  $K_d$  values at pH 5.5. To calculate intrinsic  $K_d$  values it would be necessary to take into account the protonation

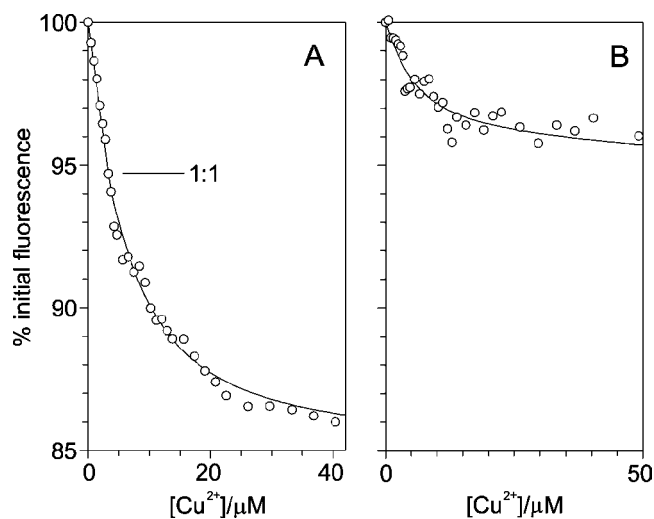


**Figure 5**  $\text{Cu}^{2+}$  binding to full-length human prion protein monitored by tryptophan fluorescence quenching

The graphs show the tryptophan fluorescence, as a percentage of the starting fluorescence, as  $\text{Cu}^{2+}$  bisglycinate is titrated into samples of  $3.5 \mu\text{M}$  prion protein at pH 5.5 in the presence of two different competition systems, (**A**) 10 mM histidine and (**B**) 100 mM histidine. The point at which one mole equivalent of  $\text{Cu}^{2+}$  has been added to the protein, and the highest affinity site is therefore saturated, is labelled 1:1 in (**A**). The lines of best fit to the binding equations (described in the Experimental section) are shown.

state of the metal binding site of the protein.). For the first binding event, the apparent dissociation constant translates to a true  $K_d$  value of  $\log_{10}(K_d/M)$  of  $-8.2 \pm 0.5$  for binding of a  $\text{Cu}^{2+}$ –mono-histidinate complex, or to  $\log_{10}(K_d/M)$  of  $-13.1 \pm 0.5$  for binding of a free  $\text{Cu}^{2+}$  ion. Despite the ambiguities, it can be concluded that the affinities of the two  $\text{Cu}^{2+}$  binding events at pH 5.5 are both in the submicromolar range and are at least an order of magnitude apart.

#### Identification of $\text{Cu}^{2+}$ co-ordinating groups in PrP<sup>91–231</sup>

The integrated nature with which all of the histidine side-chains of the N-terminal domain are involved in  $\text{Cu}^{2+}$  co-ordination in

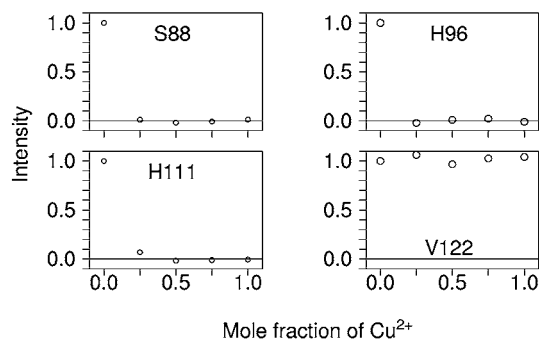


**Figure 6** Effects of titration with  $\text{Cu}^{2+}$  bisglycinate on the heights of side-chain  $[\text{C}\beta, \text{H}\beta]$  NMR signals in  $\text{PrP}^{91-231}$

Reductions induced by proximity to  $\text{Cu}^{2+}$  show the co-ordinating groups for the  $\text{Cu}^{2+}$  binding site in this truncated construct. The plots show the signal height as a fraction of its starting value during titration with  $\text{Cu}^{2+}$ .

the full-length prion protein is somewhat surprising, given that a truncated form of the protein without the octapeptide repeat regions ( $\text{PrP}^{91-231}$ ) is also capable of submicromolar affinity  $\text{Cu}^{2+}$  binding [12]. In  $\text{PrP}^{91-231}$ , the  $\text{Cu}^{2+}$  binding site was proposed to involve His<sup>96</sup> and His<sup>111</sup> on the basis of broadening of NMR signals from backbone NH moieties and X-ray absorption data [12,38]. To investigate the relationship between the two  $\text{Cu}^{2+}$  binding modes, we have carried out further characterization of the  $\text{PrP}^{91-231}$ - $\text{Cu}^{2+}$  complex under equivalent conditions to our investigation of the full-length protein.

The identity of the ligands was determined by following the titration of  $\text{Cu}^{2+}$  bisglycinate into a sample of  $^{15}\text{N}$   $^{13}\text{C}$  labelled  $\text{PrP}^{91-231}$  using heteronuclear NMR methods, as described above. After addition of 0.25 molar equivalents of  $\text{Cu}^{2+}$  to  $\text{PrP}^{91-231}$ , a specific group of  $[\text{C}, \text{H}]$  signals were completely attenuated, whilst the majority of signals, such as Val<sup>122</sup>, were unaffected by  $\text{Cu}^{2+}$  addition (Figure 6). The attenuated signals included the  $[\text{C}\beta, \text{H}\beta]$ ,  $[\text{C}\delta 2, \text{H}\delta 2]$  and  $[\text{C}\epsilon 1, \text{H}\epsilon 1]$  resonances of His<sup>96</sup> and His<sup>111</sup>. In addition, the  $[\text{C}\alpha, \text{H}\alpha]$  and  $[\text{C}\beta, \text{H}\beta]$  signals of the N-terminal Ser<sup>88</sup> also became unobservable. As in the case of our  $\text{PrP}^{23-231}$  construct, Ser<sup>88</sup> was one of three residues inserted on the N-terminal side of the  $\text{PrP}^{91-231}$  sequence to form a thrombin cleavage site. The total quenching of these signals at substoichiometric  $\text{Cu}^{2+}$  concentrations again shows that exchange of  $\text{Cu}^{2+}$  between  $\text{PrP}^{91-231}$  molecules occurs rapidly within the timescale of the NMR experiment. None of the side-chain signals for other potential ligands (namely Gln<sup>91</sup>, Thr<sup>95</sup>, Ser<sup>97</sup>, Gln<sup>98</sup>, Asn<sup>100</sup>, Ser<sup>103</sup>, Thr<sup>107</sup>, Asn<sup>108</sup>, Met<sup>109</sup> and Met<sup>112</sup>) or signals for backbone amides exhibited this complete quenching at the first addition of  $\text{Cu}^{2+}$ , thus demonstrating that at pH 5.5  $\text{PrP}^{91-231}$  co-ordinates  $\text{Cu}^{2+}$  through the two histidine imidazoles of the N-terminal region and the N-terminal amine.

In previous work, the affinity of  $\text{Cu}^{2+}$  binding in the  $\text{PrP}^{91-231}$  construct was over-estimated. The affinities reported for the interaction of the truncated prion protein constructs  $\text{PrP}^{91-231}$  (and  $\text{PrP}^{52-98}$ ) with  $\text{Cu}^{2+}$  [12] were calculated from apparent dissociation constants measured in the presence of glycine at pH 8, but this did not take into account the extent of protonation of the glycine amino group at this pH, which reduces the stability of the glycinate complex and weakens the competition for  $\text{Cu}^{2+}$ . The stepwise dissociation constants for the  $\text{Cu}^{2+}$  bisglycinate complex at pH 8 are 0.3 and 3  $\mu\text{M}$ , 40-fold greater than the absolute dissociation constants for the formation of this complex from fully deprotonated glycine, which were used in the original

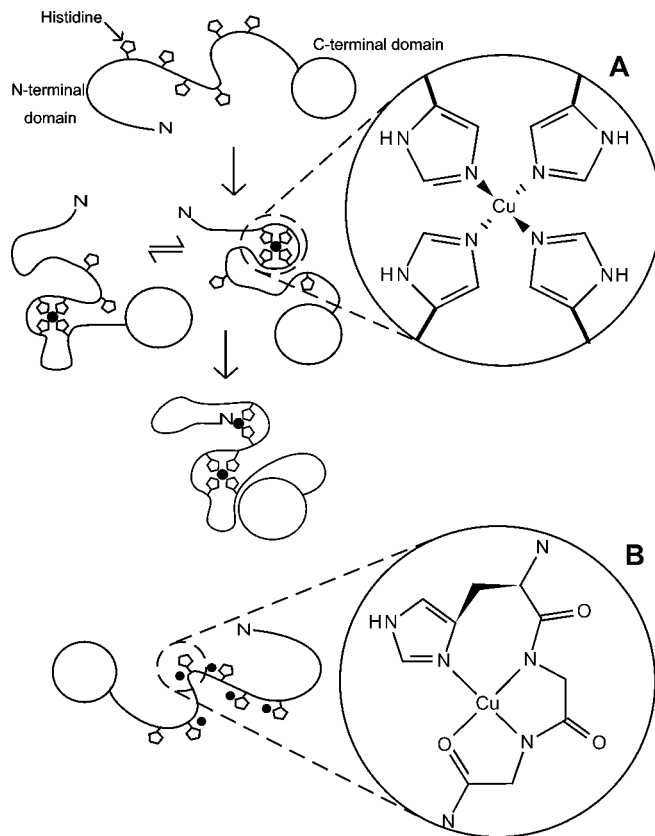


**Figure 7** An illustration of the two alternative modes of  $\text{Cu}^{2+}$  co-ordination in the full-length prion protein with details showing the co-ordination environment of the  $\text{Cu}^{2+}$  ion in each case

Binding of  $\text{Cu}^{2+}$  by the full-length prion protein at pH 5.5 involves co-ordination by an exchanging combination of histidine imidazoles (A). The Figure shows apo-PrP (top), the  $\text{PrP}-\text{Cu}^{2+}$  ensemble (middle) and  $\text{PrP}-2\text{Cu}^{2+}$  (bottom), which may also be an ensemble of different co-ordinations involving the same ligands. Note that the assignment of particular combinations of ligands to any one complex or metal centre is arbitrary. The histidine N<sup>ε</sup> co-ordination shown is based on an IR study of multiple histidine co-ordination in the octapeptide repeats [13]. At pH 7.4, with saturating concentrations of copper, the full-length prion protein can bind at least five  $\text{Cu}^{2+}$  ions, each co-ordinated by a single imidazole and nearby backbone amides (B).

calculations. When this is considered, the dissociation constant for free  $\text{Cu}^{2+}$  binding to  $\text{PrP}^{91-231}$  is in the picomolar range, with a  $\log(K_d/M)$  of  $-10.1$  and the equivalent value for  $\text{PrP}^{52-98}$  is  $-10.5$ .

## DISCUSSION

### A model of $\text{Cu}^{2+}$ binding to the full-length prion protein

A model of  $\text{Cu}^{2+}$  binding to the full-length prion protein is illustrated in Figure 7(A). The  $\text{PrP}-\text{Cu}^{2+}$  complex is an ensemble of species in which  $\text{Cu}^{2+}$  co-ordination is shared between the six histidine residues of the N-terminal domain and the N-terminal amine, with rapid exchange of ligands at the metal centre. Some fraction of the  $\text{PrP}-\text{Cu}^{2+}$  species exists as an oligomer, which is likely to simply comprise  $\text{Cu}^{2+}$  ions co-ordinated by histidine residues from more than one protein molecule. The  $\text{PrP}-2\text{Cu}^{2+}$  complex co-ordinates  $\text{Cu}^{2+}$  through total occupancy of the ligands used in the  $\text{PrP}-\text{Cu}^{2+}$  ensemble of complexes. With the present approach it cannot be determined which ligands co-ordinate each  $\text{Cu}^{2+}$  ion, and it is possible that  $\text{PrP}-2\text{Cu}^{2+}$  is also a rapidly



exchanging ensemble of species with different co-ordination modes. Although the formation of two distinct sites would be a simpler model, this cannot account for the broadening of NMR signals from all seven co-ordinating groups by the first addition of  $\text{Cu}^{2+}$  and the observation that no further signals are broadened after the 1:1 point of the titration. In the wild-type protein, lacking the three residue addition in the construct used here, co-ordination by the Ser<sup>20</sup> amine would almost certainly be replaced by the Lys<sup>23</sup> backbone amine, since the basicity of the backbone amines and the effective molarity of the two amino acids are virtually the same. The backbone amine group in lysine has a  $\text{pK}_a$  of 9.18 and the dissociation constant for formation of a 1:1  $\text{Cu}^{2+}$  complex is  $10^{-7.6}$  M, whilst for serine these values are 9.60 and  $10^{-7.9}$  M respectively [30]. The  $\text{pK}_a$  of the sidechain amine in lysine is 10.72, indicating it is far less likely to be involved in metal binding.

Here we have shown that at pH 5.5 the full-length prion protein is capable of binding two  $\text{Cu}^{2+}$  ions with co-ordination from multiple histidine imidazole groups (Figure 7A). At first, this may appear to contradict some other studies that have reported that the protein can bind five or six  $\text{Cu}^{2+}$  ions at pH 7.4 with a co-ordination involving deprotonated backbone amides [19] (Figure 7B), but the crucial difference between the experiments is the pH. The mode of  $\text{Cu}^{2+}$  co-ordination that occurs at neutral pH, with maximum  $\text{Cu}^{2+}$  occupancy, has been extensively studied. The octapeptide repeats can bind four  $\text{Cu}^{2+}$  ions, with one ion in each repeat unit, and with co-ordination of each ion by a histidine imidazole N<sup>δ1</sup>, two deprotonated backbone amides from adjacent glycine residues and a carbonyl oxygen [16].  $\text{Cu}^{2+}$  ions can also bind at two additional and independent sites, involving the residues His<sup>96</sup> and His<sup>111</sup>, again with co-ordination from the histidine imidazole and nearby backbone amides [19,26]. This brings the total number of sites to six.

However recent studies of peptides, which comprise the four repeats of the octapeptide sequence, have shown that if the peptide binds only a single  $\text{Cu}^{2+}$  ion, then co-ordination involves multiple histidine imidazole groups [24,25]. When  $\text{Cu}^{2+}$  binding in the peptide is saturated, this form of binding is replaced by the four identical sites involving backbone amides. The latter binding sites are very sensitive to reduction in pH because each involves two deprotonated backbone amide groups and the  $\text{pK}_a$  of this group is well above 7.4. In contrast, multiple histidine co-ordination would be expected to be maintained at lower pH values because the  $\text{pK}_a$  of the histidine group is around 6, and this is indeed what we observe in the full-length protein at pH 5.5.

The peptide studies of Valensin et al. [25] and Chattopadhyay et al. [24] and our own recently published work [38a], suggest that the multiple histidine  $\text{Cu}^{2+}$  co-ordination mode we observe in the full-length protein at pH 5.5 will be similar to the binding mode that occurs at neutral pH at low  $\text{Cu}^{2+}$  occupancy, even though at maximum  $\text{Cu}^{2+}$  occupancy co-ordination will be very different (Figure 7B). Consistent with this proposal EPR investigations also report that, in the presence of 1 or 2 molar equivalents of  $\text{Cu}^{2+}$  at pH 7.4,  $\text{Cu}^{2+}$  co-ordination is different to that which occurs in the  $\text{Cu}^{2+}$  saturated species [19]. It is further supported by an X-ray absorption study, which found evidence that single and multiple imidazole  $\text{Cu}^{2+}$  co-ordination might both be accessible in the full-length protein at neutral pH [39].

The affinity of the prion protein for  $\text{Cu}^{2+}$  and the availability of  $\text{Cu}^{2+}$  are the key determinants of whether the prion protein binds  $\text{Cu}^{2+}$  *in vivo*. The high capacity, backbone amide co-ordinated form of  $\text{Cu}^{2+}$  binding, which is accessible at pH 7.4, produces a substantial CD signal, and this has been used to determine that the affinity of these sites is in the low micromolar range [14]. *In vivo*, virtually all extracellular  $\text{Cu}^{2+}$  is sequestered in complexes with affinities significantly higher than micromolar, for

example with amino acids such as histidine or with proteins such as serum albumin, which have affinities in the low nanomolar and low picomolar range respectively [28,40]. A micromolar affinity therefore suggests that the cellular prion protein does not bind  $\text{Cu}^{2+}$  *in vivo*. However, the preference of the prion protein for multiple histidine  $\text{Cu}^{2+}$  co-ordination at low  $\text{Cu}^{2+}$  concentrations and at lower pH values shows that this is likely to be the highest-affinity form of binding in the protein. The affinity measurements carried out here indicate that this form of co-ordination has an affinity at least in the nanomolar range and potentially higher. While not conclusively showing that the prion protein is an authentic cuproprotein, it is clear that the multiple histidine mode of  $\text{Cu}^{2+}$  binding is the most likely to be of biological relevance. In addition, the capability for  $\text{Cu}^{2+}$  binding at pH 5.5 indicates that  $\text{Cu}^{2+}$  binding could be maintained during the cycling of the prion protein through acidic endosomal compartments [41], which have been postulated to be the site of PrP<sup>Sc</sup> formation [42].

It should be emphasized that the  $\text{Cu}^{2+}$  dependent oligomerization we observe is a distinct process from the oligomerization involved in formation of either PrP<sup>Sc</sup> or PrP fibrils. We observe association of the disordered N-terminal domain with no evidence for any structural changes in the globular C-terminal domain. In contrast, formation of PrP<sup>Sc</sup> or PrP fibrils from monomeric PrP<sup>C</sup> involves a substantial conformational change within residues 90–231, giving an increase in  $\beta$ -sheet type structure [43,44] and does not require residues 23–89 [45], which contain the octapeptide repeats. Nevertheless, our work suggests that metal binding may play a role in controlling self-association of PrP *in vivo*, which could influence the rate of formation of other PrP oligomers such as PrP<sup>Sc</sup>. Although the  $\text{Cu}^{2+}$ -dependent self-association is relatively weak at pH 5.5, requiring protein concentrations in the order of 0.5 mM, at pH 7.4 self-association is likely to be stronger. At this pH we have found that  $\text{Cu}^{2+}$  binding to a peptide comprising the four tandem octapeptide repeats causes self-association with peptide concentrations in the sub-micromolar range (M. A. Wells and G. S. Jackson, unpublished work). Also, *in vivo*, effective concentrations of the prion protein may be vastly elevated above the true concentration because the protein is anchored to the cell membrane and is further localized in cholesterol-rich lipid rafts [46], which may be sufficient to allow  $\text{Cu}^{2+}$  binding to trigger self-association.

The involvement of His<sup>96</sup> and His<sup>111</sup> in  $\text{Cu}^{2+}$  binding in the full-length protein shows that metal ion occupancy must play a role in determining the conformation of this section of the protein in the PrP<sup>C</sup> isoform, as has also been shown for PrP<sup>Sc</sup> [47]. Given the known importance of this region of the protein for prion propagation, the role of metal ions in the conversion process should be considered. The formation of a single  $\text{Cu}^{2+}$  binding site by histidine residues from the unstructured N-terminal domain also has possible implications for understanding the mechanism by which a unique group of pathogenic mutations, namely the octapeptide repeat insertion mutations, cause disease. Most of the pathogenic mutations seen in inherited prion disease occur within residues 89–231 [1], which form the relatively protease resistant core of PrP<sup>Sc</sup> and are sufficient to support prion replication and the development of pathology [45,48]. Insertional mutations comprising addition of integral numbers of the octapeptide repeat sequence to the four repeats of the wild-type protein are the exception [1]. The mechanism by which the octapeptide repeat region influences the formation of PrP<sup>Sc</sup> is unclear, especially since this section of the protein is unfolded and highly mobile in PrP<sup>C</sup>, and is rapidly digested by proteinase K in PrP<sup>Sc</sup> [49]. However the  $\text{Cu}^{2+}$  mediated interaction demonstrated here between the octapeptide repeats and His<sup>96</sup> and His<sup>111</sup>, illustrates that the insertions would cause alterations in metal co-ordination,



which have the potential to modulate PrP<sup>Sc</sup> formation by causing conformational changes within residues 91–231.

This work was funded by the U.K. Medical Research Council and the U.K. Biotechnology and Biological Sciences Research Council. We thank Clare Trevitt for assistance with protein expression and purification, Matt Cliff and Lilia Milanese for critical reading of the manuscript, Cameron McLeod and Neil Bramall for trace metal analysis of NMR samples, and Accelrys for the provision of Felix.

## REFERENCES

- Collinge, J. (2001) Prion diseases of humans and animals: Their causes and molecular basis. *Annu. Rev. Neurosci.* **24**, 519–550
- Prusiner, S. B. (1998) Prions. *Proc. Natl. Acad. Sci. U.S.A.* **95**, 13363–13383
- Griffith, J. S. (1967) Self-replication and scrapie. *Nature (London)* **215**, 1043–1044
- Prusiner, S. B. (1982) Novel proteinaceous infectious particles cause scrapie. *Science* **216**, 136–144
- Oesch, B., Westaway, D., Walchli, M., McKinley, M. P., Kent, S. B. H., Aebersold, R., Barry, R. A., Tempst, P., Teplow, D. B., Hood, L. E. et al. (1985) A cellular gene encodes scrapie Prp 27–30 protein. *Cell* **40**, 735–746
- Stahl, N., Borchelt, D. R., Hsiao, K. and Prusiner, S. B. (1987) Scrapie prion protein contains a phosphatidylinositol glycolipid. *Cell* **51**, 229–240
- Bueler, H., Fischer, M., Lang, Y., Bluethmann, H., Lipp, H. P., Dearmond, S. J., Prusiner, S. B., Aguet, M. and Weissmann, C. (1992) Normal development and behaviour of mice lacking the neuronal cell-surface Prp protein. *Nature (London)* **356**, 577–582
- Collinge, J., Whittington, M. A., Sidle, K. C. L., Smith, C. J., Palmer, M. S., Clarke, A. R. and Jefferys, J. G. R. (1994) Prion protein is necessary for normal synaptic function. *Nature (London)* **370**, 295–297
- Brown, D. R., Qin, K. F., Herms, J. W., Madlung, A., Manson, J., Strome, R., Fraser, P. E., Kruck, T., vonBohlen, A., SchulzSchaeffer, W. et al. (1997) The cellular prion protein binds copper *in vivo*. *Nature (London)* **390**, 684–687
- Hornshaw, M. P., McDermott, J. R. and Candy, J. M. (1995) Copper-binding to the N-terminal tandem repeat regions of mammalian and avian prion protein. *Biochem. Biophys. Res. Commun.* **207**, 621–629
- Hornshaw, M. P., McDermott, J. R., Candy, J. M. and Lakey, J. H. (1995) Copper-binding to the N-terminal tandem repeat region of mammalian and avian prion protein – structural studies using synthetic peptides. *Biochem. Biophys. Res. Commun.* **214**, 993–999
- Jackson, G. S., Murray, I., Hosszu, L. L. P., Gibbs, N., Waltho, J. P., Clarke, A. R. and Collinge, J. (2001) Location and properties of metal-binding sites on the human prion protein. *Proc. Natl. Acad. Sci. U.S.A.* **98**, 8531–8535
- Miura, T., Hori-i, A., Mototani, H. and Takeuchi, H. (1999) Raman spectroscopic study on the copper(II) binding mode of prion octapeptide and its pH dependence. *Biochemistry* **38**, 11560–11569
- Viles, J. H., Cohen, F. E., Prusiner, S. B., Goodin, D. B., Wright, P. E. and Dyson, H. J. (1999) Copper binding to the prion protein: structural implications of four identical cooperative binding sites. *Proc. Natl. Acad. Sci. U.S.A.* **96**, 2042–2047
- Whittal, R. M., Ball, H. L., Cohen, F. E., Burlingame, A. L., Prusiner, S. B. and Baldwin, M. A. (2000) Copper binding to octapeptide peptides of the prion protein monitored by mass spectrometry. *Protein Sci.* **9**, 332–343
- Burns, C. S., Aronoff-Spencer, E., Dunham, C. M., Lario, P., Avdievich, N. I., Antholine, W. E., Olmstead, M. M., Vrieland, A., Gerfen, G. J., Peisach, J. et al. (2002) Molecular features of the copper binding sites in the octapeptide domain of the prion protein. *Biochemistry* **41**, 3991–4001
- Garnett, A. P. and Viles, J. H. (2003) Copper binding to the octapeptides of the prion protein. Affinity, specificity, folding, and cooperativity: insights from circular dichroism. *J. Biol. Chem.* **278**, 6795–6802
- Aronoff-Spencer, E., Burns, C. S., Avdievich, N. I., Gerfen, G. J., Peisach, J., Antholine, W. E., Ball, H. L., Cohen, F. E., Prusiner, S. B. and Millhauser, G. L. (2000) Identification of the Cu<sup>2+</sup> binding sites in the N-terminal domain of the prion protein by EPR and CD spectroscopy. *Biochemistry* **39**, 13760–13771
- Burns, C. S., Aronoff-Spencer, E., Legname, G., Prusiner, S. B., Antholine, W. E., Gerfen, G. J., Peisach, J. and Millhauser, G. L. (2003) Copper co-ordination in the full-length, recombinant prion protein. *Biochemistry* **42**, 6794–6803
- Stockel, J., Safar, J., Wallace, A. C., Cohen, F. E. and Prusiner, S. B. (1998) Prion protein selectively binds copper(II) ions. *Biochemistry* **37**, 7185–7193
- Kramer, M. L., Kratzin, H. D., Schmidt, B., Romer, A., Windl, O., Liemann, S., Hornemann, S. and Kretschmar, H. (2001) Prion protein binds copper within the physiological concentration range. *J. Biol. Chem.* **276**, 16711–16719
- Zahn, R. (2003) The octapeptide repeats in mammalian prion protein constitute a pH-dependent folding and aggregation site. *J. Mol. Biol.* **334**, 477–488
- Riek, R., Hornemann, S., Wider, G., Billeter, M., Glockshuber, R. and Wuthrich, K. (1996) NMR structure of the mouse prion protein domain PrP(121–321). *Nature (London)* **382**, 180–182
- Chattopadhyay, M., Walter, E. D., Newell, D. J., Jackson, P. J., Aronoff-Spencer, E., Peisach, J., Gerfen, G. J., Bennett, B., Antholine, W. E. and Millhauser, G. L. (2005) The octapeptide domain of the prion protein binds Cu(II) with three distinct co-ordination modes at pH 7.4. *J. Am. Chem. Soc.* **127**, 12647–12656
- Valensin, D., Luczkowski, M., Mancini, F. M., Legowska, A., Gaggelli, E., Valensin, G., Rolka, K. and Kozlowski, H. (2004) The dimeric and tetrameric octapeptide fragments of prion protein behave differently to its monomeric unit. *Dalton Trans.* 1284–1293
- Jones, C. E., Klewpatinond, M., Abdelraheim, S. R., Brown, D. R. and Viles, J. H. (2005) Probing copper<sup>2+</sup> binding to the prion protein using diamagnetic nickel<sup>2+</sup> and <sup>1</sup>H NMR: the unstructured N terminus facilitates the co-ordination of six copper<sup>2+</sup> ions at physiological concentrations. *J. Mol. Biol.* **346**, 1393–1407
- Jones, C. E., Abdelraheim, S. R., Brown, D. R. and Viles, J. H. (2004) Preferential Cu<sup>2+</sup> co-ordination by His<sup>96</sup> and His<sup>111</sup> induces  $\beta$ -sheet formation in the unstructured amyloidogenic region of the prion protein. *J. Biol. Chem.* **279**, 32018–32027
- Linder, M. C. (1991) Extracellular copper substituents and mammalian copper transport. In *Biochemistry of Copper* (Linder, M. C., ed.), pp. 73–134, Plenum Press, New York
- Hosszu, L. L. P., Jackson, G. S., Trevitt, C. R., Jones, S., Batchelor, M., Bhelt, D., Prodromidou, K., Clarke, A. R., Waltho, J. P. and Collinge, J. (2004) The residue 129 polymorphism in human prion protein does not confer susceptibility to Creutzfeldt–Jakob disease by altering the structure or global stability of PrP<sup>C</sup>. *J. Biol. Chem.* **279**, 28515–28521
- Jackson, G. S., Hill, S. F., Joseph, C., Hosszu, L., Power, A., Waltho, J. P., Clarke, A. R. and Collinge, J. (1999) Multiple folding pathways for heterologously expressed human prion protein. *BBA-Protein Struct. M.* **1431**, 1–13
- Gill, S. C. and Vonhippel, P. H. (1989) Calculation of protein extinction coefficients from amino-acid sequence data. *Anal. Biochem.* **182**, 319–326
- Bertini, I., Luchinat, C. and Parigi, G. (2001) Nuclear relaxation due to dipolar coupling with unpaired electrons. In *Solution NMR of Paramagnetic Molecules*. pp. 89–96, Elsevier, Amsterdam
- Dawson, R. M. C., Elliott, D. C., Elliott, W. H. and Jones, K. M. (1986) Stability constants for metal complexes. In *Data for Biochemical Research*. (Dawson, R. M. C., ed.), pp. 399–416, Oxford University Press, Oxford
- Shriver, D. F., Atkins, P. W. and Langford, C. H. (1994) *Inorganic Chemistry*. Oxford University Press, Oxford
- Wilkinson, G., Gillard, R. D. and McCleverty, J. (1987) Stability of complexes. In *Comprehensive Co-ordination Chemistry* (Wilkinson, G., Gillard, R. D. and McCleverty, J., eds.), p. 526, Pergamon, Oxford
- Reference deleted
- Bertini, I., Luchinat, C. and Parigi, G. (2001) Metal centred point-dipole approximation. In *Solution NMR of Paramagnetic Molecules*, pp. 37–42, Elsevier, Amsterdam
- Hasnain, S. S., Murphy, L. M., Strange, R. W., Grossmann, J. G., Clarke, A. R., Jackson, G. S. and Collinge, J. (2001) XAFS study of the high-affinity copper-binding site of human PrP<sup>91–231</sup> and its low-resolution structure in solution. *J. Mol. Biol.* **311**, 467–473
- Wells, M. A., Jelinska, C., Hosszu, L. L. P., Craven, C. J., Clarke, A. R., Collinge, J., Waltho, J. P. and Jackson, G. S. (2006) Multiple forms of copper (II) co-ordination occur throughout the N-terminal region of the prion protein at pH 7.4. *Biochem. J.* Immediate publication doi 10.1042/BJ20060721
- Morante, S., Gonzalez-Iglesias, R., Patrich, C., Meneghini, C., Meyer-Klaucke, W., Menestrina, G. and Gasset, M. (2004) Inter- and intra-octapeptide Cu(II) site geometries in the prion protein – implications in Cu(II) binding cooperativity and Cu(II)-mediated assemblies. *J. Biol. Chem.* **279**, 11753–11759
- Masuoka, J., Hegenauer, J., Vandyke, B. R. and Saltman, P. (1993) Intrinsic stoichiometric equilibrium – constants for the binding of zinc(II) and copper(II) to the high-affinity site of serum-albumin. *J. Biol. Chem.* **268**, 21533–21537
- Shyng, S. L., Huber, M. T. and Harris, D. A. (1993) A Prion Protein Cycles between the Cell-Surface and an Endocytic Compartment in Cultured Neuroblastoma-Cells. *J. Biol. Chem.* **268**, 15922–15928
- Mayer, R. J., Landon, M., Laszlo, L., Lennox, G. and Lowe, J. (1992) Protein processing in lysosomes: the new therapeutic target in neurodegenerative disease. *Lancet* **340**, 156–159
- Pan, K. M., Baldwin, M., Nguyen, J., Gasset, M., Serban, A., Groth, D., Mehlhorn, I., Huang, Z. W., Fletterick, R. J., Cohen, F. E. and Prusiner, S. B. (1993) Conversion of  $\alpha$ -helices into  $\beta$ -sheets features in the formation of the scrapie prion proteins. *Proc. Natl. Acad. Sci. U.S.A.* **90**, 10962–10966
- Baskakov, I. V., Legname, G., Gryczynski, Z. and Prusiner, S. B. (2004) The peculiar nature of unfolding of the human prion protein. *Protein Sci.* **13**, 586–595
- Rogers, M., Yehieli, F., Scott, M. and Prusiner, S. B. (1993) Conversion of truncated and elongated prion proteins into the scrapie isoform in cultured cells. *Proc. Natl. Acad. Sci. U.S.A.* **90**, 3182–3186

- 46 Vey, M., Pilkuhn, S., Wille, H., Nixon, R., DeArmond, S. J., Smart, E. J., Anderson, R. G., Taraboulos, A. and Prusiner, S. B. (1996) Subcellular colocalization of the cellular and scrapie prion proteins in caveolae-like membranous domains. *Proc. Natl. Acad. Sci. U.S.A.* **93**, 14945–14949
- 47 Wadsworth, J. D. F., Hill, A. F., Joiner, S., Jackson, G. S., Clarke, A. R. and Collinge, J. (1999) Strain-specific prion-protein conformation determined by metal ions. *Nat. Cell Biol.* **1**, 55–59
- 48 Fischer, M., Rulicke, T., Raeber, A., Sailer, A., Moser, M., Oesch, B., Brandner, S., Aguzzi, A. and Weissmann, C. (1996) Prion protein (PrP) with amino-proximal deletions restoring susceptibility of PrP knockout mice to scrapie. *EMBO J.* **15**, 1255–1264
- 49 Prusiner, S. B., Groth, D. F., Bolton, D. C., Kent, S. B. and Hood, L. E. (1984) Purification and structural studies of a major scrapie prion protein. *Cell* **38**, 127–134

---

Received 28 March 2006/22 June 2006; accepted 6 July 2006

Published as BJ Immediate Publication 6 July 2006, doi:10.1042/BJ20060458